



# Arabidopsis IRE1 catalyses unconventional splicing of *bZIP60* mRNA to produce the active transcription factor

Yukihiro Nagashima<sup>1</sup>, Kei-ichiro Mishiba<sup>1</sup>, Eiji Suzuki<sup>1</sup>, Yukihiro Shimada<sup>2</sup>, Yuji Iwata<sup>3,4</sup>  
& Nozomu Koizumi<sup>1</sup>

SUBJECT AREAS:

ARABIDOPSIS

GENE EXPRESSION

RNA

SIGNAL TRANSDUCTION

Received  
28 April 2011

Accepted  
8 June 2011

Published  
1 July 2011

Correspondence and requests for materials should be addressed to N.K. (nkoizumi@plant.osakafu-u.ac.jp)

<sup>1</sup>Graduate School of Life and Environmental Sciences, Osaka Prefecture University, 1-1 Gakuencho, Nakaku, Sakai, Osaka, 599-8531, Japan, <sup>2</sup>Kihara Institute for Biological Research, Yokohama City University, Maiokacho 641-12, Totsuka, Yokohama, Kanagawa, 244-0813, Japan, <sup>3</sup>Biology Department and Huck Institutes of the Life Sciences, Pennsylvania State University, 211 Wartik, University Park, PA 16802, USA, <sup>4</sup>Division of Chemical and Life Sciences and Engineering, King Abdullah University of Science and Technology, Thuwal 23955-6900, Kingdom of Saudi Arabia.

**IRE1 plays an essential role in the endoplasmic reticulum (ER) stress response in yeast and mammals. We found that a double mutant of Arabidopsis *IRE1A* and *IRE1B* (*ire1a/ire1b*) is more sensitive to the ER stress inducer tunicamycin than the wild-type. Transcriptome analysis revealed that genes whose induction was reduced in *ire1a/ire1b* largely overlapped those in the *bzip60* mutant. We observed that the active form of *bZIP60* protein detected in the wild-type was missing in *ire1a/ire1b*. We further demonstrated that *bZIP60* mRNA is spliced by ER stress, removing 23 ribonucleotides and therefore causing a frameshift that replaces the C-terminal region of *bZIP60* including the transmembrane domain (TMD) with a shorter region without a TMD. This splicing was detected in *ire1a* and *ire1b* single mutants, but not in the *ire1a/ire1b* double mutant. We conclude that IRE1A and IRE1B catalyse unconventional splicing of *bZIP60* mRNA to produce the active transcription factor.**

In eukaryotic cells, proteins synthesised in the endoplasmic reticulum (ER) are appropriately folded and assembled before leaving the ER. If these processes are disturbed, unfolded proteins accumulate in the ER and the signalling pathway from the ER to the nucleus is activated to induce the transcription of genes encoding the ER protein quality control molecules, such as molecular chaperones, folding enzymes and components of ER-associated protein degradation as well as other stress related proteins. This cellular response conserved in eukaryotes is referred to as the unfolded protein response or the ER stress response<sup>1, 2</sup>.

IRE1 plays an essential role in the signalling pathway of the ER stress response in yeast. IRE1 is an ER-resident type I transmembrane protein with a sensor domain in its luminal side and kinase and RNase domains in its cytoplasmic side. When sensing ER stress, IRE1 oligomerises and transactivates its RNase activity by autophosphorylation through its kinase activity<sup>3</sup>. Dissociation of BiP from the sensor domain triggers this oligomerisation<sup>4</sup>, whereas the sensor domain itself is considered to recognise unfolded proteins<sup>5</sup>. The activated RNase domain cleaves 2 specific phosphodiester bonds in *HAC1* mRNA that encodes a *bZIP* transcription factor<sup>6, 7</sup>. After cleavage, 5' and 3' fragments of *HAC1* mRNA are joined by the tRNA ligase Rlg1<sup>8</sup>. Splicing removes 252 nucleotides from the precursor mRNA *HAC1u* to generate the spliced *HAC1* mRNA *HAC1s*. *HAC1s* encodes *HAC1s* protein consisting of 238 amino acids, which is larger than the *HAC1u* protein (230 amino acids). The *HAC1s* protein contains an 18-amino acid sequence that is important for transcription factor activity, which is missing in the *HAC1u* protein<sup>9</sup>.

Two *IRE1* homologues, *IRE1α* and *IRE1β*, have been identified in mammalian cells. Mammalian *IRE1α* is considered to be a functional homologue of yeast *IRE1* because *IRE1α* catalyses unconventional splicing of *XBPI* mRNA in a manner analogous to its yeast counterpart<sup>10</sup>. In this case, splicing removes a 26-nucleotide segment, which is much shorter than the *HAC1* mRNA intron. Nevertheless, yeast *HAC1* and human *XBPI* share a secondary structural feature around the splicing sites i.e. both *HAC1* and *XBPI* mRNAs have 2 stem-loop structures with conserved ribonucleotides in the 7-nucleotide loops<sup>10, 11</sup>. The precursor *XBPI* mRNA (*XBPIu*) encodes an *XBPIu* protein of 261 amino acids; however, because of a frameshift caused by splicing, the spliced *XBPI* mRNA (*XBPIs*) produces the *XBPIs* protein of 376 amino acids with a different and longer amino acid sequence at the C-terminus. As in the case of the *HAC1s* protein, the *XBPIs* protein gains a transcriptional



activator domain in the new C-terminal region<sup>10,11</sup>. Mammalian cells have 2 additional ER stress sensors: the membrane-bound transcription factor ATF6 and the receptor-type protein kinase PERK. ATF6 is anchored to the ER membrane by virtue of its transmembrane domain (TMD) and is activated by proteolysis mediated by the proteases S1P and S2P<sup>12,13</sup>.

In plants, 2 *IRE1* homologues, *IRE1A* and *IRE1B*, have been reported in Arabidopsis (*Arabidopsis thaliana*)<sup>14,15</sup>. Both *IRE1A* and *IRE1B* are localised in the ER and their putative sensor domains function as an actual sensor in yeast<sup>15</sup>. However, their involvement in the ER stress response remains to be determined. Similar to yeast and mammalian cells, Arabidopsis *IRE1A* and *IRE1B* may also catalyse unconventional splicing of a certain mRNA: however, such an mRNA is yet to be identified.

Arabidopsis also has stress transducers similar to those of mammals. bZIP17 and bZIP28 have a TMD, as does ATF6, and are therefore considered to be activated by proteolysis mediated by the proteases S1P and S2P<sup>16–18</sup>. bZIP60 was identified as a bZIP transcription factor whose transcript is induced by treatment with tunicamycin, an inhibitor of N-linked glycosylation widely used to induce the ER stress response<sup>19</sup>. bZIP60 encodes 295-amino acid protein that consists of a transcriptional activation domain, bZIP domain, putative TMD and C-terminal region<sup>19,20</sup>. Induction of several tunicamycin-inducible genes was reduced in the *bzip60* mutant, providing evidence that bZIP60 is involved in transcriptional activation of ER stress-inducible genes<sup>21</sup>.

Several experiments were performed to elucidate the underlying mechanism of bZIP60 activation. First, a transient expression assay showed that expression of bZIP60 $\Delta$ C, an artificial truncated form of bZIP60 whose TMD and C-terminal region were deleted, activated promoters of ER chaperone genes, whereas expression of the native form of bZIP60 did not<sup>19</sup>. Second, an immunoblot analysis using an antibody raised against bZIP60 $\Delta$ C showed that in addition to the native form of bZIP60, a faster-migrating, smaller form of bZIP60 existed and was present only when plants were treated with tunicamycin<sup>21</sup>. Third, a subcellular fractionation experiment showed that the native and smaller forms of bZIP60 were localised to the ER and the nucleus, respectively<sup>21</sup>. On the basis of these observations, it was hypothesized that the bZIP60 protein is bound to the ER membrane through its TMD and is cleaved in response to ER stress, thereby producing the nuclear-localised, active bZIP60<sup>21,22</sup>. However, the molecular basis of bZIP60 activation has been enigmatic because neither S1P nor S2P appear to be involved in the production of the active form of bZIP60 protein<sup>21</sup>. In the current study, we present evidence that the active form of bZIP60 protein is synthesised from mRNA spliced by *IRE1A* and *IRE1B*.

## Results

**A double mutant of *IRE1* homologues exhibited tunicamycin sensitivity.** T-DNA insertion mutants of Arabidopsis *IRE1A* (*ire1a*) and *IRE1B* (*ire1b*) were obtained from stock centres of T-DNA insertion lines (Fig. 1a). We generated *ire1a* and *ire1b* single mutants as well as an *ire1a/ire1b* double mutant (Fig. 1b and Supplementary Fig. S1 online, see Methods section for nomenclature of *IRE1* genes and their mutants). All of these mutants were visibly indistinguishable from wild-type plants under ambient laboratory conditions grown on soil. However, when their seeds were sown on medium containing various concentrations of tunicamycin, germination of the *ire1a/ire1b* double mutant was more severely inhibited than that of the wild-type and single mutants (Fig. 1c, d and Supplementary Fig. S2 online), implying the involvement of both *IRE1A* and *IRE1B* in the ER stress response.

Differences in sensitivity against tunicamycin might be due to a decreased transcriptional induction of a gene encoding UDP-N-acetylglucosamine:dolichol phosphate N-acetylglucosamine-1-P transferase (GPT), an enzyme that catalyses the initial step of the

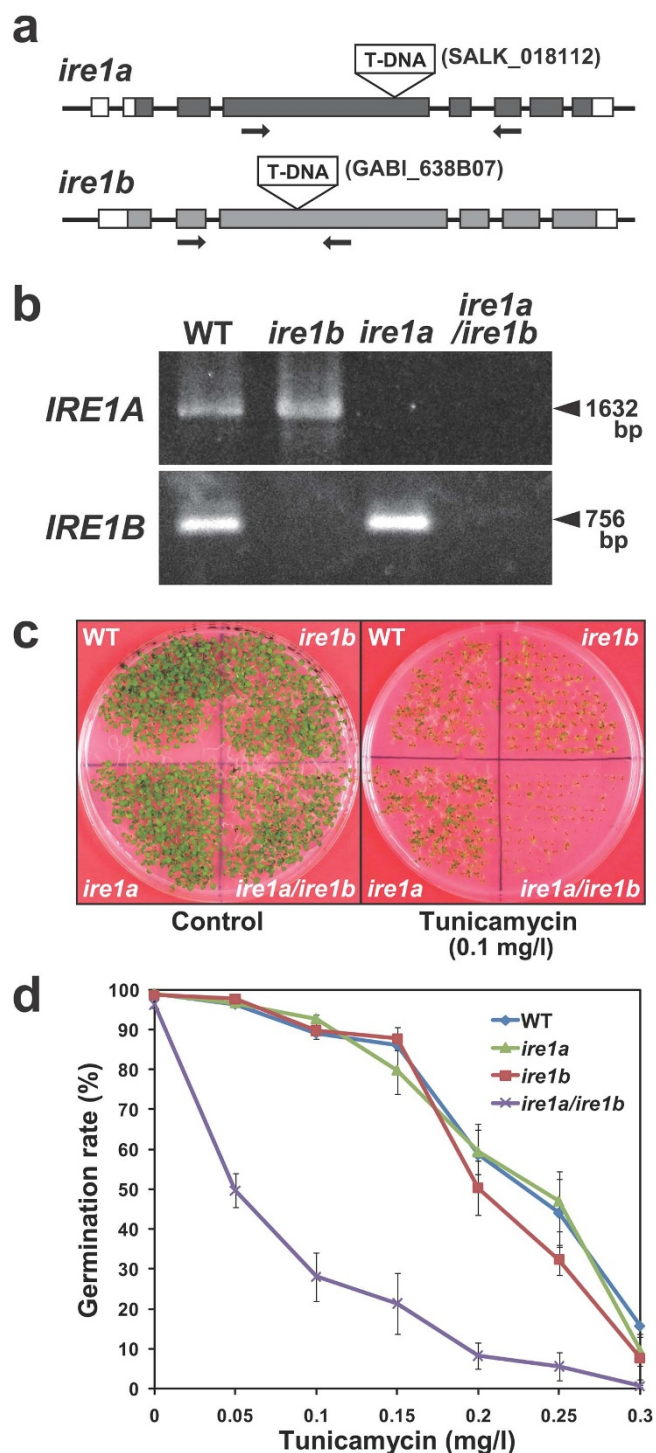


**Figure 1 | Different sensitivities of T-DNA insertion mutants of *IRE1* homologues toward tunicamycin.** a, Schematic representation of T-DNA insertion sites in *ire1a* and *ire1b*. Grey and white boxes indicate coding sequences and untranslated regions, respectively. b, RT-PCR analysis of wild-type, *ire1a*, *ire1b* and *ire1a/ire1b* mutants. RT-PCR analysis was performed using primers depicted in a. c, Tunicamycin sensitivity of wild-type and *ire1* mutants. Seeds of wild-type (WT), *ire1a*, *ire1b* and *ire1a/ire1b* were sown on MS medium with or without tunicamycin (0.1 mg/l). A picture was taken 2 weeks after sowing. d, Effect of different concentrations of tunicamycin on germination of wild-type and *ire1* mutant seeds. The same experiment was performed as in c with different concentrations of tunicamycin. Data are expressed as the mean  $\pm$  SE of 3 independent experiments.



N-linked glycan biosynthetic pathway and whose activity is inhibited by tunicamycin. This inference is based on the fact that in our previous study, an increased expression of *GPT* conferred resistance to tunicamycin<sup>23</sup>. Therefore we analysed *GPT* expression in *ire1* mutants. Induction of *GPT* was not affected in any of the *ire1* mutants (Supplementary Fig. S3 online).

**Genes whose induction was reduced in *ire1a/ire1b* largely overlapped those in *bzip60*.** To investigate how ER stress-inducible genes are affected in the *ire1a/ire1b* double mutant, seedlings of the wild-type and *ire1a/ire1b* were mock or tunicamycin treated and subjected to transcriptome analysis using a microarray representing approximately 24,000 genes in Arabidopsis. A hybridisation signal of 162 genes was increased 2.5-fold or more at 5 h of tunicamycin treatment in the wild-type with P value of less than 0.05 (see Methods for details) (Supplementary Table S1 online). Of these, 59 genes showed 50% or less induction by tunicamycin treatment in *ire1a/ire1b* than that in the wild-type, indicating that *IRE1s* are involved in the induction of the ER stress-inducible genes, although we could not exclude the possibility that the difference in the level of transcript accumulation between wild-type and *ire1a/ire1b* plants is due to a different mRNA turnover rate.

Our previous transcriptome analysis revealed that several genes are less induced in response to tunicamycin treatment in *bzip60* mutant plants<sup>21</sup>. To investigate how IRE1-dependent and -independent genes are affected in *bzip60*, we compared the pattern of tunicamycin induction in *ire1a/ire1b* with that in *bzip60*. We first retrieved the list of tunicamycin-inducible genes in wild-type and *bzip60* plants from our previous study<sup>21</sup>. After selecting 81 genes that were present in both the current and the previous gene lists (Supplementary Table S2 online), we performed a hierarchical cluster analysis using fold induction values in wild-type and *ire1a/ire1b* plants obtained from the current study, along with those in wild-type and *bzip60* plants from the previous study<sup>21</sup>. As shown in Fig. 2a, induction of a considerable number of tunicamycin-inducible genes (63 out of 81 genes; approximately 80%) was similarly affected in both *ire1a/ire1b* and *bzip60* mutant plants i.e. a majority of genes whose induction was reduced in *ire1a/ire1b* showed reduced induction in *bzip60* (see Group II genes in Fig. 2a), whereas genes whose induction was unaffected in *ire1a/ire1b* also tended to be unaffected in *bzip60* (see Group III genes in Fig. 2a). It should be noted that a certain proportion of genes showed even higher induction by tunicamycin treatment in *ire1a/ire1b* than in the wild-type (see Group I genes in Fig. 2a), as is evident by fold induction values in *ire1a/ire1b* divided by those in the wild-type being much greater than 1; no such difference was observed between the wild-type and *bzip60*.

The selected genes were subjected to RNA blot analysis. As shown in Fig. 2b, inductions of *BiP3* and *Sar1* were clearly reduced in *ire1a/ire1b*, whereas induction of *BiP1* was still observed in *ire1a/ire1b*. This result was reminiscent of the pattern of transcriptional induction observed in *bzip60*<sup>21</sup>. A reduced induction of these genes was not observed in the *ire1a* or *ire1b* single mutant (Fig. 2c, Supplementary Fig. S3 online). This result was consistent with the observation that the *ire1a/ire1b* double mutant was much more sensitive to tunicamycin than the wild-type or the single mutants.

**The active form of bZIP60 protein was absent in *ire1a/ire1b*.** Our observation that IRE1A/IRE1B and bZIP60 share a similar set of transcriptional targets suggested that IRE1A/IRE1B and bZIP60 are involved in the same signalling pathway. As an initial approach to clarify their relationship, we monitored the expression profile of *bZIP60* in *ire1a/ire1b*. As shown in Fig. 3a, transcripts of *bZIP60* accumulated by tunicamycin treatment in both the wild-type and *ire1a/ire1b* although induction was slightly weaker in *ire1a/ire1b*, which is consistent with the hybridisation signals obtained from the microarray analysis (see Supplementary Table S2 online).

Subsequently, we performed immunoblot analysis using anti-bZIP60 antibody to examine the level of the active form of bZIP60 protein in *ire1a/ire1b*. The active, nuclear-localised form of bZIP60 protein migrating faster on an SDS-PAGE gel<sup>21</sup> was detected by tunicamycin treatment in the wild-type but not in *ire1a/ire1b* (Fig. 3b). The active form of bZIP60 was detected in both *ire1a* and *ire1b* single mutants (Fig. 3c), suggesting that both IRE1A and IRE1B are involved in the production of the active form of bZIP60 protein. In addition to tunicamycin, DTT treatment also induced the active form of bZIP60 protein in the wild-type but not in *ire1a/ire1b* (Fig. 3d). The active form of bZIP60 protein that appeared in response to tunicamycin and DTT treatments was slightly larger than bZIP60 $\Delta$ C transiently expressed in protoplasts (Fig. 3d).

**The conserved stem-loop structures essential for the splicing by IRE1 were found in *bZIP60* mRNA.** On the basis of the aforementioned observations, we hypothesized that *bZIP60* mRNA is regulated by unconventional splicing catalysed by IRE1A and IRE1B in a manner similar to the regulation of *HAC1* and *XBPI* mRNAs. Therefore we predicted the *bZIP60* mRNA secondary structure using the CentroidFold software (<http://www.ncrna.org/>)<sup>24</sup>. As shown in Fig. 4a and Supplementary Fig. S4 online, *bZIP60* mRNA probably forms 2 stem-loop structures observed in *HAC1* and *XBPI* mRNAs<sup>10, 11</sup>. The conserved nucleotides in both of the 7-nucleotide loops essential for *HAC1* and *XBPI* mRNA splicing<sup>10, 11</sup> were also observed in *bZIP60* mRNA, except that the second loop consisted of 8 instead of 7 nucleotides (Fig. 4a). Based on the splicing rule conserved in *HAC1* and *XBPI*, we predicted that the 23-nucleotide intron is spliced out from *bZIP60* mRNA during the ER stress response (Fig. 4b). We designated the unspliced and spliced mRNAs as *bZIP60u* and *bZIP60s*, respectively.

*bZIP60s* was predicted to produce a smaller protein (Fig. 4c, d and Supplementary Fig. S5 online), i.e. *bZIP60u* encodes a protein of 295 amino acids, whereas *bZIP60s* encodes a protein of 258 amino acids. The frameshift due to the 23-nucleotide splicing generates a new, different amino acid sequence (ORF2) in the C-terminal region of the bZIP60s protein. By converting from bZIP60u to bZIP60s, the bZIP60 protein loses the TMD that has been considered to anchor bZIP60u to the ER membrane. This estimation is consistent with the electrophoretic mobility of proteins observed in Fig. 3d in comparison to that of bZIP60 $\Delta$ C, which is an artificially truncated form encoding a protein of 216 amino acids<sup>19</sup>.

BLAST searches detected sequences homologous to *bZIP60* in 16 plant species. Alignment of their nucleotide sequences around the possible splicing site showed that the 6 nucleotides considered to be important for splicing were completely conserved, whereas amino acid sequences were not necessarily conserved (Supplementary Fig. S6 online). A putative intron is 23 nucleotides long in dicots, whereas it is 20 nucleotides long in monocots such as rice. A few EST sequences corresponding to a spliced form were found in currently available databases. We were unable to find any sequence corresponding to *bZIP60s* in Arabidopsis EST databases.

***bZIP60s* was detected by tunicamycin treatment in the wild-type but not in *ire1a/ire1b*.** To test the above hypothesis, RNA was prepared from wild-type and *ire1a/ire1b* plants treated with tunicamycin and subjected to RT-PCR amplification using primers designed to detect an amplicon including the predicted intron (Fig. 5a). A smaller band of predicted size was detected by tunicamycin treatment in the wild-type but not in *ire1a/ire1b* (Fig. 5b). This band was cloned into a plasmid vector and subjected to sequencing. The determined sequence was the same as that predicted in Fig. 4.

Subsequently, primers were designed to anneal specifically to *bZIP60s* (Fig. 5a) and used for RT-PCR amplification. As shown in Fig. 5c, the amplicon of the predicted size was detected by tunicamycin treatment in the wild-type, but again not in *ire1a/ire1b*. This

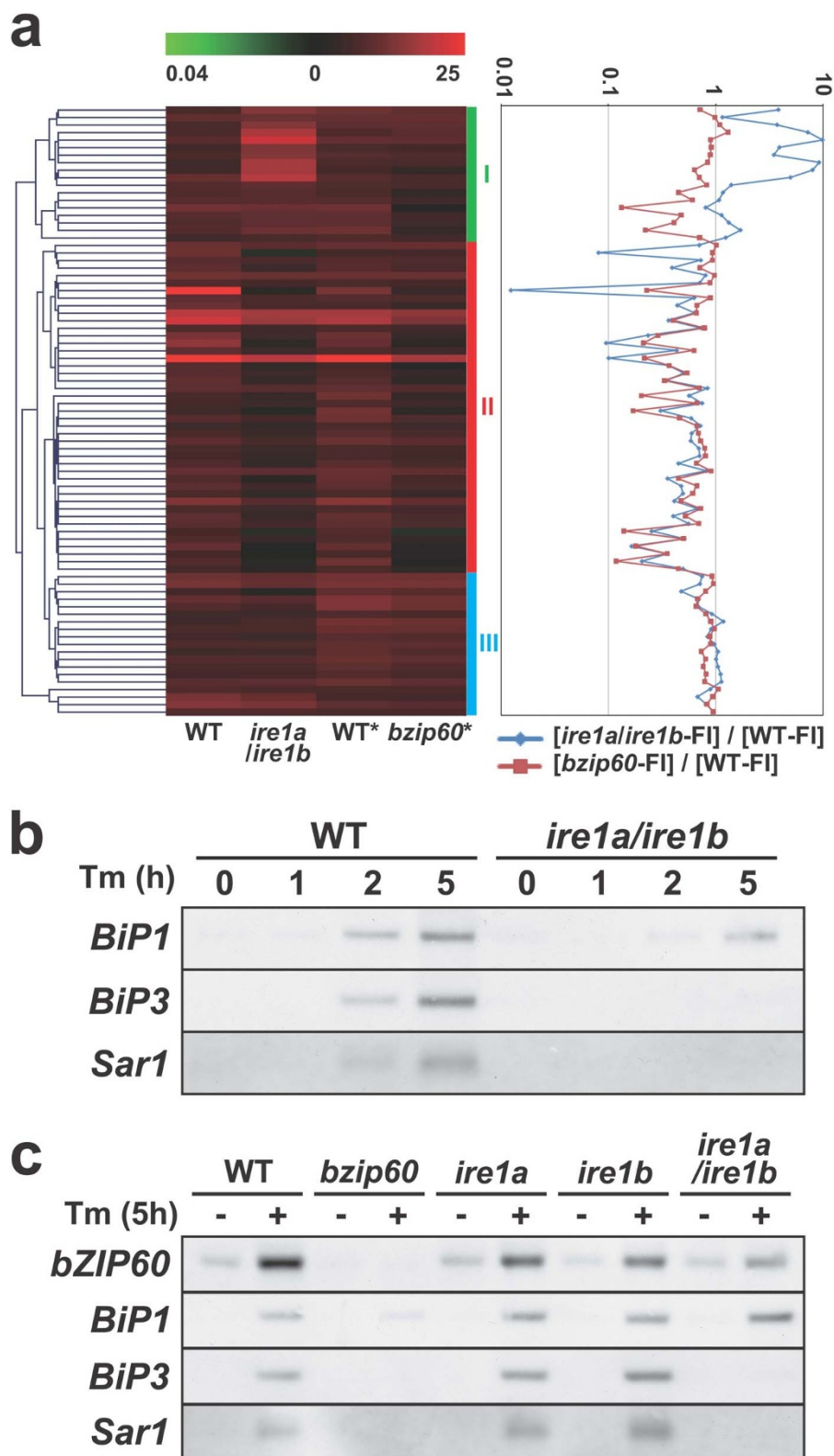


**Figure 2** | Expression profile of tunicamycin-inducible genes in the wild-type and *ire1a/ire1b* and *bzip60* mutants. **a**, Hierarchical cluster analysis of wild-type and mutant plants. A hierarchical cluster analysis was performed using fold induction values of tunicamycin-inducible genes in wild-type and *ire1a/ire1b* plants along with those in wild-type and *bzip60* plants retrieved from the study by Iwata *et al.*<sup>21</sup>, which were indicated by asterisks. Each horizontal bar represents a fold induction value of a given mRNA. On the right is a graph where a fold induction value of *ire1a/ire1b* was divided by that of wild-type plants and plotted on a logarithmic scale with blue. The same plot was made in red by using fold induction values of the wild-type and *bzip60* retrieved from the study by Iwata *et al.*<sup>21</sup> with regard to Groups I, II and III, see the main text for the explanation. **b**, Time course induction of *BiP1*, *BiP3* and *Sar1* by tunicamycin in the wild-type (WT) and *ire1a/ire1b*. It should be noted that the *BiP1* probe also detects *BiP2*. Seedlings were treated with 5 mg/l tunicamycin for indicated time periods. RNA was extracted and subjected to RNA blot analysis. **c**, Induction of *BiP1*, *BiP3* and *Sar1* by tunicamycin treatment in *bzip60* and *ire1* mutants. Seedlings were treated with 5 mg/l tunicamycin for 5 h. RNA was extracted and subjected to RNA blot analysis.

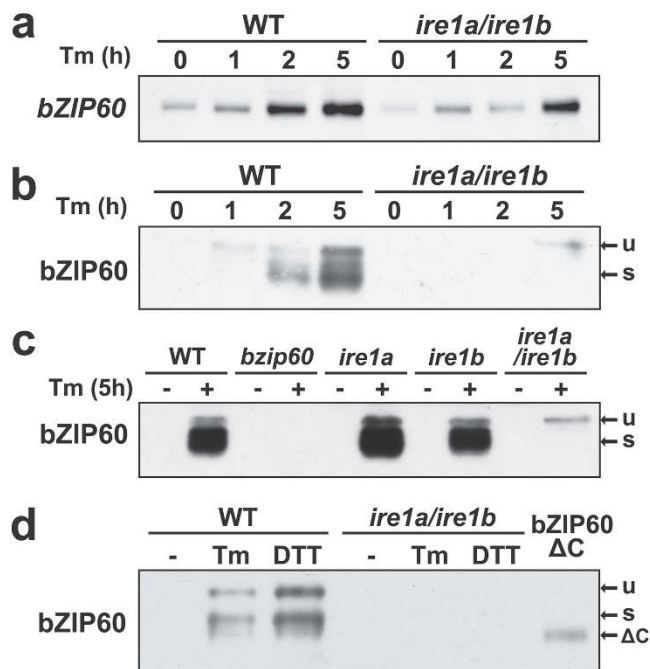


**Figure 3 | Induction of *bZIP60* mRNA and activation of bZIP60 protein in the wild-type and *ire1* mutants.** a, RNA blot analysis of *bZIP60* in the wild-type and *ire1a/ire1b* treated with tunicamycin. RNA was prepared from seedlings treated with tunicamycin (5 mg/l) for the indicated period. b, Immunoblot analysis of bZIP60 in the wild-type and *ire1a/ire1b*. Protein extracts were prepared from seedlings treated as in a, and immunoblot analysis was performed using anti-bZIP60 antibody. Ten micrograms of total protein was loaded in each lane. c, Immunoblot analysis of bZIP60 in the wild-type, *bzip60*, *ire1a*, *ire1b* and *ire1a/ire1b*. Seedlings treated with tunicamycin (5 mg/l) or DMSO (0.1%) as a control for 5 h were subjected to immunoblot analysis as in b. d, Immunoblot analysis of bZIP60 in the wild-type and in *ire1a/ire1b* by tunicamycin and DTT treatments. Seedlings were treated with DMSO (0.1%; -), tunicamycin (5 mg/l; Tm) and DTT (2 mM) for 5 h and used for protein extraction. bZIP60 $\Delta$ C was transiently expressed in protoplasts prepared from *bzip60* mutants and used for immunoblot analysis alongside. Positions of bZIP60u (u), bZIP60s (s) and bZIP60 $\Delta$ C ( $\Delta$ C) are indicated.

amplification did not appear to be affected in either of the *ire1a* or *ire1b* single mutant (Fig. 5d), indicating that both IRE1A and IRE1B are involved in the splicing of *bZIP60* mRNA.

## Discussion

In the current study we provide evidence that Arabidopsis IRE1 homologues are involved in the ER stress response through unconventional splicing of *bZIP60* mRNA. We first showed that the *ire1a/ire1b* double mutant, but not the *ire1a* or *ire1b* single mutant, is much more sensitive to tunicamycin than the wild-type. Microarray analysis demonstrated that induction of several tunicamycin-inducible genes is less pronounced in *ire1a/ire1b* than in the wild-type. Strikingly, a majority of those genes were also less induced in the *bzip60* mutant. We further showed that the *ire1a/ire1b* double mutant does not accumulate the active form of the bZIP60 protein even when treated with tunicamycin. We noticed that *bZIP60* mRNA has a secondary structure that is possibly subject to splicing by IRE1. This structure is strictly conserved in at least 16 *bZIP60* homologues in plants. In particular, 6 nucleotides that have been shown to be essential in yeast *HAC1* and mammalian *XBP1*<sup>10, 11</sup> are completely conserved even though the corresponding amino acid sequences are not necessarily conserved, indicating the importance of this RNA secondary structure. We revealed that splicing of *bZIP60* mRNA

actually occurs in response to tunicamycin treatment. In addition, we demonstrated that *bZIP60* mRNA splicing and the subsequent production of the active form of bZIP60 protein are dependent on both IRE1A and IRE1B.

We had previously concluded that bZIP60 is activated by proteolysis near the TMD in a manner similar to mammalian ATF6 and plant bZIP28<sup>21</sup>. This model arose from the fact that bZIP60 has a putative TMD (amino acids 224–244) after the bZIP domain (amino acids 140–197), and the truncated form bZIP60 $\Delta$ C (amino acids 1–216) activated promoters of ER stress-inducible genes<sup>19</sup>. Our model was also supported by the observation that bZIP60u, which we previously called the full-length form, was detected in the ER fraction whereas bZIP60s, which we previously called the cleaved form, was detected in the nuclear fraction<sup>21</sup>. Importantly, however, in this study we showed that the apparent molecular mass of bZIP60s is considerably larger than that of bZIP60 $\Delta$ C (Fig. 4d). Our current model nicely explains this size difference, because bZIP60u, bZIP60s and bZIP60 $\Delta$ C encode proteins of 295, 258 and 216 amino acids, respectively.

Our current model is also supported by the existence of cDNA sequences of *bZIP60* homologues in other plant species that lack the predicted intron (Supplementary Fig. S6 online). The boundary sequences of the intron are highly conserved among *bZIP60* homologues. Most strikingly, the 3 nucleotides in both the first and second loops of 7 nucleotides essential for *HAC1* and *XBP1* mRNA splicing<sup>10, 11</sup> are strictly conserved, except that the second loop is of 8 rather than 7 nucleotides in plant *bZIP60* homologues, thus indicating that the RNA secondary structure with the conserved ribonucleotides is essential for IRE1-dependent splicing. It is worth mentioning that RT-PCR analysis using primers amplifying both *bZIP60u* and *bZIP60s* detected much less *bZIP60s* than *bZIP60u* (Fig. 5b). This could be attributed to a stable secondary structure that *bZIP60s* might form, making it resistant to transcription by a reverse transcriptase. Alternatively, the spliced mRNA could actually be a minor entity *in vivo*.

Although some regulation of a transcription factor through unconventional splicing by IRE1 appears to also be conserved in plants, a clear difference exists in terms of the underlying molecular basis when compared to yeast and mammalian counterparts (see Fig. 6). First, although both mammals and Arabidopsis have 2 *IRE1* paralogues, Arabidopsis *IRE1A* and *IRE1B* are functionally redundant in terms of *bZIP60* mRNA splicing, whereas mammalian *IRE1 $\alpha$*  and *IRE1 $\beta$*  have distinct functions, i.e. the former catalyses the unconventional splicing and the latter catalyses 28S ribosomal RNA cleavage<sup>10, 25</sup>. Most notably, in marked contrast to yeast and mammals where *HAC1s* and *XBP1s* gain a transcriptional activation domain at their C-terminus after splicing<sup>9, 10</sup>, bZIP60u already contains a transcriptional activation domain at its N-terminus<sup>20</sup>. In this regard, it is interesting to note that the XBP1u protein acts as a negative regulator<sup>26</sup>. It has been reported that a nuclear export signal and a signal for protein degradation are present only in the XBP1u protein at the C-terminal region, and that the XBP1u protein forms a heterodimer with XBP1s and exports it to the cytoplasm for proteasome-dependent degradation. This is believed to downregulate the amount of XBP1s protein that needs to be degraded in the absence of ER stress. However, the same may not hold true for bZIP60u because it needs to be excluded from the nucleus in the absence of ER stress because of the presence of a transcriptional activation domain in its N-terminal region. This exclusion of bZIP60u from the nucleus is probably attributed to the TMD that anchors bZIP60u to the ER membrane, as experimentally verified in our previous study<sup>21</sup>.

Recently, Yanagitani *et al.* reported that the XBP1u protein tends to localise to the ER membrane through a hydrophobic region (HR) in its C-terminal region<sup>27</sup>. This anchoring of the XBP1u protein recruits *XBP1u* mRNA to the ER membrane where IRE1 $\alpha$  localises and is therefore considered to achieve efficient splicing of *XBP1u*. A

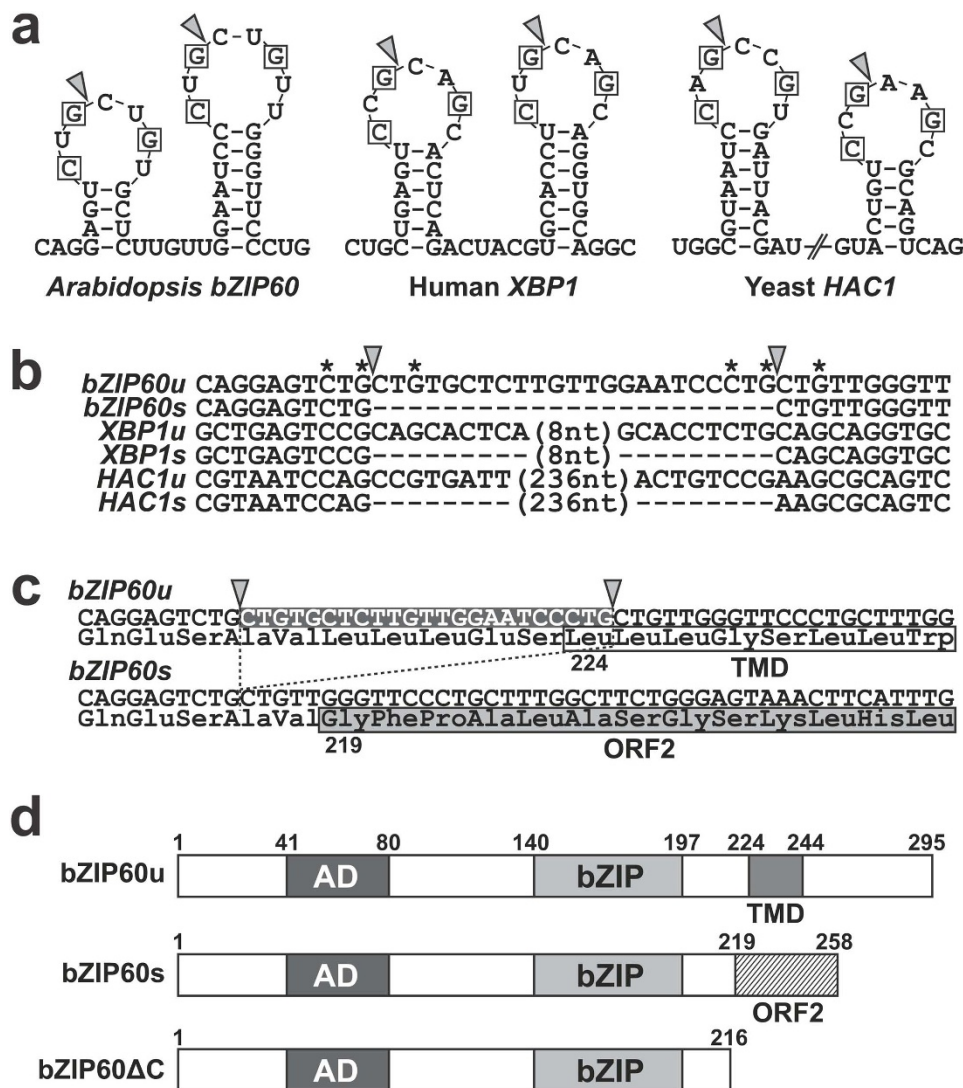


**Figure 4** | Prediction of unconventional splicing of *bZIP60* mRNA. **a**, Stem-loop structures observed in *bZIP60*, *XBP1* and *HAC1* mRNA. The conserved nucleotides essential for splicing of *HAC1* and *XBP1* mRNAs are indicated in boxes. The corresponding nucleotides conserved in *bZIP60* mRNA are also indicated in boxes. Triangles indicate the splicing sites observed in *HAC1* and *XBP1* mRNAs, as well as the sites predicted in *bZIP60* mRNA. **b**, Nucleotide sequence alignment of unspliced and spliced *bZIP60*, *HAC1* and *XBP1* cDNA around the splicing sites. Asterisks and triangles indicate the conserved nucleotides and the splicing sites, respectively. **c**, Nucleotide and deduced amino acid sequences around the splicing sites of *bZIP60* cDNA. The splicing sites are indicated by triangles. The amino acid sequence corresponding to the putative TMD is indicated by an unshaded box and the sequence translated after splicing was indicated by a shaded box as ORF2. Complete sequences of *bZIP60u* and *bZIP60s* are presented in Supplementary Fig. S5 online. **d**, Schematic representations of *bZIP60u*, *bZIP60s* and *bZIP60ΔC*. The transcriptional activation domain is indicated by AD.

similar mechanism could be considered for *bZIP60* because the TMD of *bZIP60* is located immediately after the 23-nucleotide intron and the TMD gets deleted by the frameshift caused by splicing (Fig. 4c). Therefore, the putative TMD of *bZIP60* might be an HR binding to the periphery of the membrane rather than a peptide region spanning the lipid bilayer. If the scenario for *XBP1* is applied to *bZIP60*, the C-terminal region of *bZIP60u* may have an amino acid sequence responsible for the attenuation of translation that allows sufficient time for IRE1 to catalyse splicing<sup>28</sup>. A moderately conserved amino acid sequence in the C-terminal region of *bZIP60u* in several plant species might be of functional relevance for *bZIP60* mRNA splicing.

It is worth mentioning that the transcriptome response of tunicamycin-inducible genes in *ire1a/ire1b* is not exactly the same as that in *bzip60*, i.e. although a majority of tunicamycin-inducible genes whose induction is reduced in *ire1a/ire1b* are also reduced in *bzip60*, a certain proportion of genes show even higher induction in

*ire1a/ire1b* than in the wild-type whereas no such genes are observed between the wild-type and *bzip60* (see Group I genes in Fig. 2a). This implies that IRE1 is not solely dedicated to splicing-mediated *bZIP60* activation, but also affects other molecules. Indeed, besides an unconventional splicing of mRNA encoding a transcription factor, mammalian IRE1 has been shown to mediate mRNA decay, 28S ribosomal RNA cleavage and activation of ASK1, a mediator of ER stress-induced apoptosis<sup>25, 29–31</sup>.

During the preparation of this manuscript, Deng *et al.* reported the splicing of *bZIP60* mRNA<sup>32</sup>. Their RT-PCR analysis using *ire1* single mutants suggests that only IRE1B accounts for splicing. However, given the differences in the tunicamycin sensitivity and in the levels of *bZIP60* mRNA splicing and *bZIP60s* protein among the *ire1* single and double mutants observed in the current study, it is evident that both IRE1A and IRE1B catalyse the unconventional splicing of *bZIP60* mRNA in response to ER stress and cause a frameshift, leading to the production of the active *bZIP60* transcription factor.

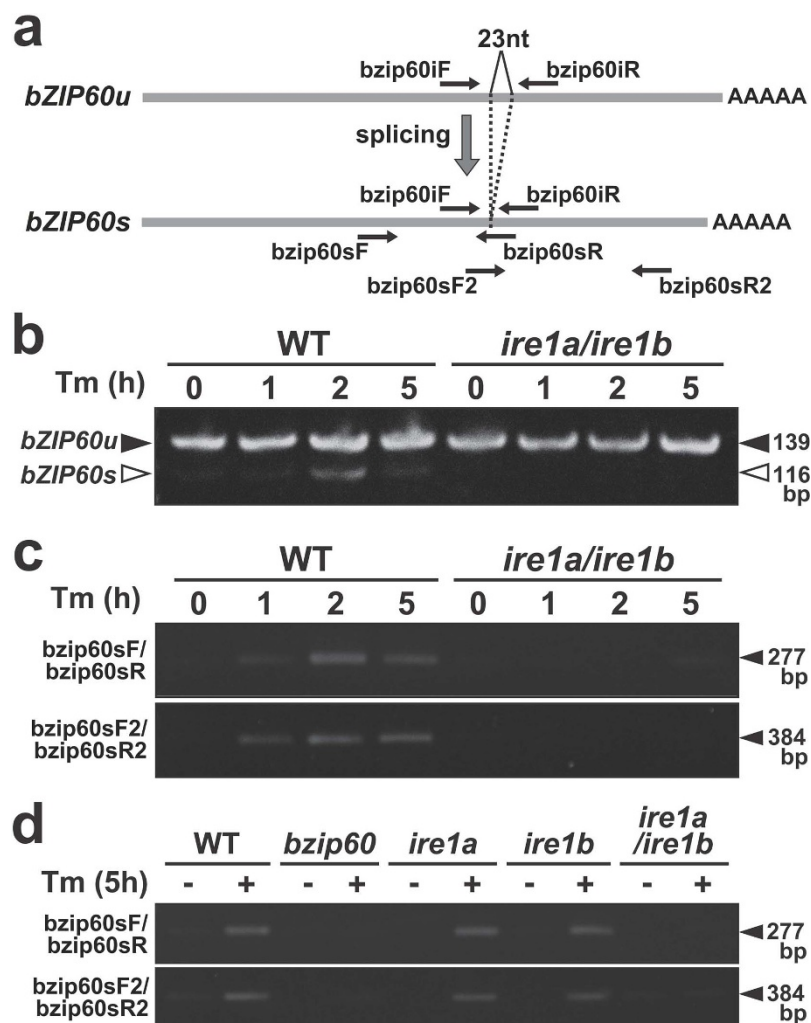


**Figure 5 | Detection of the unconventional splicing of *bZIP60* mRNA.** a, Schematic representation of primer locations used for detection of unconventional splicing. The locations of primers for detecting both *bZIP60u* and *bZIP60s*, as well as the ones for specifically detecting *bZIP60s*, are indicated. b, Detection of *bZIP60u* and *bZIP60s* cDNA. Seedlings of the wild-type and *ire1a/ire1b* treated with 5 mg/l tunicamycin for indicated time periods were used for RNA preparation. PCR amplification was performed using the primer set bzip60iF/bzip60iR. c, Detection of *bZIP60s* cDNA in the wild-type and *ire1a/ire1b*. PCR amplification was performed using 2 primer sets, bzip60sF/bzip60sR and bzip60sF2/bzip60sR2, with the same RNA preparation as in b. d, Detection of *bZIP60s* cDNA in the wild-type, *bzip60*, *ire1a*, *ire1b* and *ire1a/ire1b*. RNA was extracted from seedlings of the wild-type, *bzip60*, *ire1a* and *ire1b* single mutants and *ire1a/ire1b* double mutant treated with tunicamycin (5 mg/l; +) or DMSO (0.1%; -), and subjected to RT-PCR amplification as in c.

## Methods

**Plant material.** T-DNA insertion mutants of *Arabidopsis thaliana* *IRE1A* (SALK\_018112) and *IRE1B* (GABI\_638B07) were obtained from ABRC and GABI-Kat, respectively<sup>33, 34</sup>. A T-DNA insertion mutant of *bZIP60* (SALK\_050203) was described previously<sup>21</sup>. These mutants and the wild-type used in this study are all in Col-0 background. Two insertion mutants (*ire1a* and *ire1b*) were crossed and the double mutant (*ire1a/ire1b*) was isolated from their progenies. Insertion of a T-DNA and its homozygosity were confirmed by PCR using genomic DNA and by RT-PCR as shown in Fig. 1b and Supplementary Fig. S1 online.

**Nomenclature of *IRE1* genes and their T-DNA insertion mutants.** There are 2 independently published reports that refer to 2 *Arabidopsis* *IRE1* homologues (AGI codes At2g17520 and At5g24360) using different names; At2g17520 and At5g24360 are referred to as *IRE1-2* and *IRE1-1*, respectively, in one report<sup>15</sup>, whereas in the other report these are referred to as *IRE1A* and *IRE1B*, respectively<sup>14</sup>. We adopted the latter naming according to widely accepted nomenclature that is followed by the *Arabidopsis* research community, whose details can be found in the TAIR website (<http://www.arabidopsis.org/>).

With regard to the *ire1* mutants, Lu and Christopher reported 3 mutants for *IRE1A* (*ire1a-1*, *ire1a-2* and *ire1a-3*) and one mutant for *IRE1B* (*ire1b-2*)<sup>35</sup>. *ire1a-2* is a T-DNA insertion mutant generated at the SALK Institute (line number; SALK\_018112) and the same line was used in this study, although we independently obtained the seeds and isolated the homozygous mutant. *IRE1B* has been reported to be essential for embryo development as inferred from the observation that *ire1b-2*

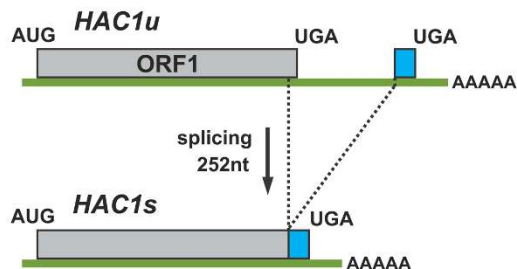
homozygous mutants could not be obtained<sup>35</sup>. We were also unable to isolate *ire1b-2* homozygotes. However, it is important to note that introducing a genomic DNA fragment containing the *IRE1B* gene did not complement the lethality of the disruption of the *IRE1B* gene (i.e. *ire1b-2* homozygotes could not be obtained even after the *IRE1B* gene was introduced). Meanwhile, we obtained another T-DNA insertion mutant from GABI-Kat and were able to isolate the homozygous mutant, which we designated as *ire1b-1*. In the current study, we used *ire1a-2* and *ire1b-1* for detailed analyses, but for simplicity in the main text we designated them as *ire1a* and *ire1b*, respectively, and the double mutant as *ire1a/ire1b*.

**Stress treatments.** To examine tunicamycin sensitivity, approximately 100 seeds of each genotype were sown on MS plates containing various concentrations of tunicamycin. Two weeks later, the percentage of germinating seeds was calculated. We considered a seedling with opened cotyledons as a germinated seed. Calculations were performed using data from 3 independent experiments.

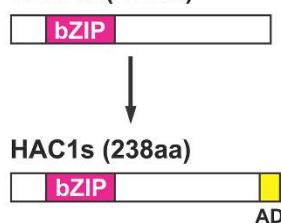
For RNA and protein extractions, sterilized seeds were sown in half-strength MS medium with 1% sucrose and allowed to grow for 10 days in a 16 h light and 8 h dark cycle at 22°C with gentle shaking. Seedlings were treated with dimethylsulfoxide (DMSO; 0.1%) as mock treatment, tunicamycin (5 mg/l), or dithiothreitol (DTT; 2 mM) for indicated time periods and subjected to RNA and protein preparation. Although this concentration of tunicamycin eventually kills seedlings, in the time range we used in the current study, we could observe a clear transcriptomic change characteristic of the ER stress response, which is indicative of an active cellular response.



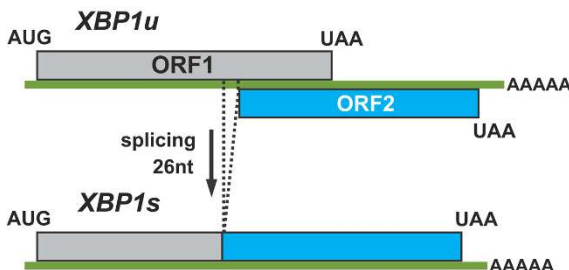
## Yeast HAC1



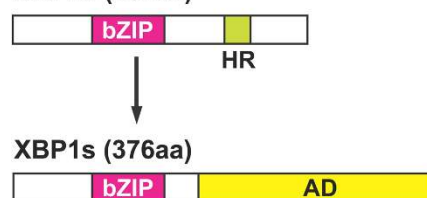
## HAC1u (230aa)



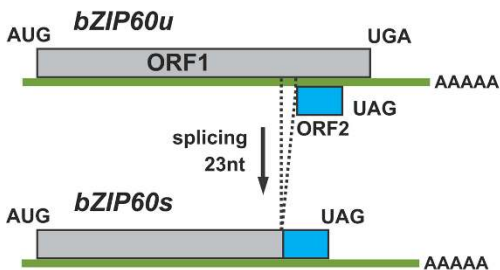
## Human XBP1



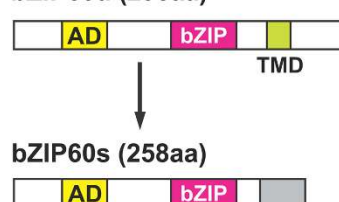
## XBP1u (261aa)



## Arabidopsis bZIP60



## bZIP60u (295aa)



**mRNA**

**Protein**

**Figure 6** | Comparison of the mRNA splicing of *HAC1*, *XBP1* and *bZIP60* and its consequences for their protein products. Details can be found in the main text.

**Microarray analysis.** The GeneChip Arabidopsis ATH1 Genome Array (Affymetrix) representing approximately 24,000 genes was used. Seedlings of the wild-type and *ire1a/ire1b* grown for 10 days were treated with either tunicamycin (5 mg/l) or DMSO (0.1%) as a solvent control for 5 h and subjected to RNA preparation. RNA was extracted using RNeasy Plant Mini Kit (Qiagen) according to the manufacturer's instructions. The experiment was performed with three biological replicates. GeneChip analyses were conducted as previously described<sup>36</sup> with the following modifications: cRNA labelling and hybridisation were conducted using the 3'IN V Express kit along with the Hybridisation, Wash and Stain kit (Affymetrix) as per the manufacturer's instructions. The signal values and detection P-values were calculated using GeneChip Operating Software (Affymetrix). The data were then transformed to log scale and then statistical analyses were conducted using R as described previously<sup>36</sup>. A false discovery rate, or FDR, was analysed as described by Storey and Tibshirani<sup>37</sup>. Microarray data can be found in the ArrayExpress database (<http://www.ebi.ac.uk/arrayexpress/>) under the accession number E-MEXP-3186 "ire1 double mutant vs wild-type in response to tunicamycin".

For the hierarchical cluster analysis, the list of tunicamycin-inducible genes in the wild-type and *bzip60* plants was retrieved from our previous publication<sup>21</sup>. Among 81 genes that are present both in the current and previous gene lists (Supplementary Table S2 online), fold induction values for wild-type and *ire1a/ire1b* plants obtained from the current study, as well as those in wild-type and *bzip60* plants from our previous study<sup>21</sup>, were calculated. The hierarchical cluster analysis was performed using MeV (<http://www.tm4.org/mev/>)<sup>38, 39</sup>. Furthermore, a fold induction value obtained from either *ire1a/ire1b* or *bzip60* plants was divided by that obtained from the corresponding wild-type plants and plotted in a graph format on a logarithmic scale.

**Quantitative RT-PCR.** RNA was extracted by using RNeasy Plant Mini Kit (Qiagen) according to the manufacturer's instructions. Quantitative RT-PCR was performed as previously described<sup>40</sup> using primers listed in Supplementary Table S3 online.

**RNA blot.** For RNA blot analysis, RNA was extracted according to the method described by Chomczynski *et al.*<sup>41</sup>. RNA blot was conducted by using the PCR DIG Probe Synthesis Kit (Roche) according to the manufacturer's instructions. Probes were prepared by PCR using the primers listed in Supplementary Table S3 online. RNA (5 µg per lane) was fractionated on a 1.5% agarose gel containing 2% formaldehyde, capillary blotted onto a nylon membrane (Biodyne PLUS, Pall Corporation) in 20× standard saline citrate (1×SSC = 0.15 M sodium chloride/0.015 M sodium citrate, pH7) and fixed by UV irradiation. The membrane was washed twice each with 1×SSC/0.1% SDS and 0.1×SSC/0.2% SDS at 68 °C, and then exposed to x-ray film.

**RT-PCR to detect *bZIP60s*.** RNA was extracted by using RNeasy Plant Mini Kit (Qiagen) according to the manufacturer's instructions. Reverse transcription was conducted at 70 °C using ThermoScript (Invitrogen). PCR was then performed at an annealing temperature of 63 °C using primers *bzip60iF* and *bzip60iR*, at 68 °C using primers *bzip60sF* and *bzip60sR* and at 64 °C using primers *bzip60sF2* and *bzip60sR2*.

**Protein analysis.** Protein extraction was performed as previously described<sup>21</sup>. Immunoblotting was performed using anti-bZIP60 antibody raised against bacterially expressed bZIP60ΔC as previously described<sup>21</sup>.





**Transient expression of bZIP60ΔC.** A plasmid harbouring bZIP60ΔC under the CaMV 35S promoter was transfected in protoplasts prepared from mature leaves of the *bzip60* mutant plants according to Iwata *et al.*<sup>22</sup>.

**Prediction of RNA secondary structure and protein domains.** The secondary structure of *bZIP60u* mRNA was predicted using CentroidFold (<http://www.ncrna.org/centroidfold/>)<sup>24</sup>. The bZIP domain and TMD of bZIP60 were predicted according to PROSITE (<http://expasy.org/prosite/>)<sup>43</sup> and TMPred ([http://www.ch.embnet.org/software/TMPRED\\_form.html](http://www.ch.embnet.org/software/TMPRED_form.html)), respectively.

**Alignment of bZIP60 homologues.** The cDNA sequences of the Arabidopsis *bZIP60u* or *bZIP60s* were queried against the nucleotide collection and expressed sequence tag databases at the National Center for Biotechnology Information using BLASTn (<http://blast.ncbi.nlm.nih.gov/Blast.cgi>). Multiple alignments of the nucleotide sequences of unspliced and spliced forms of *bZIP60* homologues were generated using ClustalW implemented in MEGA4<sup>44</sup>.

- Ron, D. & Walter, P. Signal integration in the endoplasmic reticulum unfolded protein response. *Nat Rev Mol Cell Biol* **8**, 519–529 (2007).
- Vitale, A. & Boston, R. S. Endoplasmic reticulum quality control and the unfolded protein response: insights from plants. *Traffic* **9**, 1581–1588 (2008).
- Shamu, C. E. & Walter, P. Oligomerization and phosphorylation of the Ire1p kinase during intracellular signaling from the endoplasmic reticulum to the nucleus. *EMBO J* **15**, 3028–3039 (1996).
- Kimata, Y., Oikawa, D., Shimizu, Y., Ishiwata-Kimata, Y. & Kohno, K. A role for Bip as an adaptor for the endoplasmic reticulum stress-sensing protein Ire1. *J Cell Biol* **167**, 445–456 (2004).
- Kimata, Y. *et al.* Two regulatory steps of ER-stress sensor Ire1 involving its cluster formation and interaction with unfolded proteins. *J Cell Biol* **179**, 75–86 (2007).
- Mori, K., Kawahara, T., Yoshida, H., Yanagi, H. & Yura, T. Signalling from endoplasmic reticulum to nucleus: transcription factor with a basic-leucine zipper motif is required for the unfolded protein-response pathway. *Genes Cells* **1**, 803–817 (1996).
- Cox, J. S. & Walter, P. A novel mechanism for regulating activity of a transcription factor that controls the unfolded protein response. *Cell* **87**, 391–404 (1996).
- Sidrauski, C. & Walter, P. The transmembrane kinase Ire1p is a site-specific endonuclease that initiates mRNA splicing in the unfolded protein response. *Cell* **90**, 1031–1039 (1997).
- Mori, K., Ogawa, N., Kawahara, T., Yanagi, H. & Yura, T. mRNA splicing-mediated C-terminal replacement of transcription factor Hac1p is required for efficient activation of the unfolded protein response. *Proc Natl Acad Sci USA* **97**, 4660–4665 (2000).
- Yoshida, H., Matsui, T., Yamamoto, A., Okada, T. & Mori, K. XBP1 mRNA is induced by ATF6 and spliced by IRE1 in response to ER stress to produce a highly active transcription factor. *Cell* **107**, 881–891 (2001).
- Kawahara, T., Yanagi, H., Yura, T. & Mori, K. Unconventional splicing of HAC1/ERN4 mRNA required for the unfolded protein response. Sequence-specific and non-sequential cleavage of the splice sites. *J Biol Chem* **273**, 1802–1807 (1998).
- Ye, J. *et al.* ER stress induces cleavage of membrane-bound ATF6 by the same proteases that process SREBPs. *Mol Cell* **6**, 1355–1364 (2000).
- Haze, K., Yoshida, H., Yanagi, H., Yura, T. & Mori, K. Mammalian transcription factor ATF6 is synthesized as a transmembrane protein and activated by proteolysis in response to endoplasmic reticulum stress. *Mol Biol Cell* **10**, 3787–3799 (1999).
- Noh, S. J., Kwon, C. S. & Chung, W. I. Characterization of two homologs of Ire1p, a kinase/endoribonuclease in yeast, in Arabidopsis thaliana. *Biochim Biophys Acta* **1575**, 130–134 (2002).
- Koizumi, N. *et al.* Molecular characterization of two Arabidopsis Ire1 homologs, endoplasmic reticulum-located transmembrane protein kinases. *Plant Physiol* **127**, 949–962 (2001).
- Liu, J. X., Srivastava, R., Che, P. & Howell, S. H. An endoplasmic reticulum stress response in Arabidopsis is mediated by proteolytic processing and nuclear relocation of a membrane-associated transcription factor, bZIP28. *Plant Cell* **19**, 4111–4119 (2007).
- Tajima, H., Iwata, Y., Iwano, M., Takayama, S. & Koizumi, N. Identification of an Arabidopsis transmembrane bZIP transcription factor involved in the endoplasmic reticulum stress response. *Biochem Biophys Res Commun* **374**, 242–247 (2008).
- Che, P. *et al.* Signaling from the endoplasmic reticulum activates brassinosteroid signaling and promotes acclimation to stress in Arabidopsis. *Sci Signal* **3**, ra69 (2010).
- Iwata, Y. & Koizumi, N. An Arabidopsis transcription factor, AtbZIP60, regulates the endoplasmic reticulum stress response in a manner unique to plants. *Proc Natl Acad Sci USA* **102**, 5280–5285 (2005).
- Iwata, Y., Yoneda, M., Yanagawa, Y. & Koizumi, N. Characteristics of the nuclear form of the Arabidopsis transcription factor AtbZIP60 during the endoplasmic reticulum stress response. *Biosci Biotechnol Biochem* **73**, 865–869 (2009).

- Iwata, Y., Fedoroff, N. V. & Koizumi, N. Arabidopsis bZIP60 is a proteolysis-activated transcription factor involved in the endoplasmic reticulum stress response. *Plant Cell* **20**, 3107–3121 (2008).
- Iwata, Y., Fedoroff, N. V. & Koizumi, N. The Arabidopsis membrane-bound transcription factor AtbZIP60 is a novel plant-specific endoplasmic reticulum stress transducer. *Plant Signal Behav* **4**, 514–516 (2009).
- Koizumi, N., Ujino, T., Sano, H. & Chrispeels, M. J. Overexpression of a gene that encodes the first enzyme in the biosynthesis of asparagine-linked glycans makes plants resistant to tunicamycin and obviates the tunicamycin-induced unfolded protein response. *Plant Physiol* **121**, 353–361 (1999).
- Hamada, M., Kiryu, H., Sato, K., Mituyama, T. & Asai, K. Prediction of RNA secondary structure using generalized centroid estimators. *Bioinformatics* **25**, 465–473 (2009).
- Iwakaki, T. *et al.* Translational control by the ER transmembrane kinase/ribonuclease IRE1 under ER stress. *Nat Cell Biol* **3**, 158–164 (2001).
- Yoshida, H., Oku, M., Suzuki, M. & Mori, K. pXBP1(U) encoded in XBP1 pre-mRNA negatively regulates unfolded protein response activator pXBP1(S) in mammalian ER stress response. *J Cell Biol* **172**, 565–575 (2006).
- Yanagitani, K. *et al.* Cotranslational targeting of XBP1 protein to the membrane promotes cytoplasmic splicing of its own mRNA. *Mol Cell* **34**, 191–200 (2009).
- Yanagitani, K., Kimata, Y., Kadokura, H. & Kohno, K. Translational pausing ensures membrane targeting and cytoplasmic splicing of XBP1u mRNA. *Science* **331**, 586–589 (2011).
- Hollien, J. & Weissman, J. S. Decay of endoplasmic reticulum-localized mRNAs during the unfolded protein response. *Science* **313**, 104–107 (2006).
- Hollien, J. *et al.* Regulated Ire1-dependent decay of messenger RNAs in mammalian cells. *The Journal of cell biology* **186**, 323–331 (2009).
- Nishitoh, H. *et al.* ASK1 is essential for endoplasmic reticulum stress-induced neuronal cell death triggered by expanded polyglutamine repeats. *Genes Dev* **16**, 1345–1355 (2002).
- Deng, Y. *et al.* Heat induces the splicing by IRE1 of a mRNA encoding a transcription factor involved in the unfolded protein response in Arabidopsis. *Proc Natl Acad Sci USA* **108**, 7247–7252 (2011).
- Alonso, J. M. *et al.* Genome-wide insertional mutagenesis of Arabidopsis thaliana. *Science* **301**, 653–657 (2003).
- Rosso, M. G. *et al.* An Arabidopsis thaliana T-DNA mutagenized population (GABI-Kat) for flanking sequence tag-based reverse genetics. *Plant Mol Biol* **53**, 247–259 (2003).
- Lu, D. P. & Christopher, D. A. Endoplasmic reticulum stress activates the expression of a sub-group of protein disulfide isomerase genes and AtbZIP60 modulates the response in Arabidopsis thaliana. *Mol Genet Genomics* **280**, 199–210 (2008).
- Goda, H. *et al.* The AtGenExpress hormone and chemical treatment data set: experimental design, data evaluation, model data analysis and data access. *Plant J* **55**, 526–542 (2008).
- Storey, J. D. & Tibshirani, R. Statistical significance for genomewide studies. *Proc Natl Acad Sci USA* **100**, 9440–9445 (2003).
- Saeed, A. I. *et al.* TM4 microarray software suite. *Methods Enzymol* **411**, 134–193 (2006).
- Saeed, A. I. *et al.* TM4: a free, open-source system for microarray data management and analysis. *BioTechniques* **34**, 374–378 (2003).
- Iwata, Y., Sakiyama, M., Lee, M. H. & Koizumi, N. Transcriptomic response of Arabidopsis thaliana to tunicamycin-induced endoplasmic reticulum stress. *Plant Biotechnol* **27**, 161–171 (2010).
- Chomczynski, P. & Sacchi, N. The single-step method of RNA isolation by acid guanidinium thiocyanate-phenol-chloroform extraction: twenty-something years on. *Nat Prot* **1**, 581–585 (2006).
- Iwata, Y., Lee, M. H. & Koizumi, N. Analysis of a transcription factor using transient assay in Arabidopsis protoplasts, in *Plant Transcription Factors*, Vol. 754. (eds L. Yuan & S. E. Perry) (Humana Press, in press).
- Sigrist, C. J. *et al.* PROSITE, a protein domain database for functional characterization and annotation. *Nucleic Acids Res* **38**, D161–166 (2010).
- Tamura, K., Dudley, J., Nei, M. & Kumar, S. MEGA4: Molecular Evolutionary Genetics Analysis (MEGA) software version 4.0. *Mol Biol Evol* **24**, 1596–1599 (2007).

## Acknowledgements

We thank ABRC and GABI-Kat for providing T-DNA insertion lines. We also thank TAIR for the gene annotation data used in the present study. We thank Chitose Takahashi, Sanae Tashiro, Akiko Sato and Sachiko Ooyama for technical assistance in GeneChip analysis, and Naoko Miya and Masayo Sakiyama for technical assistance in isolation of *ire1* mutants. This work was supported by Ministry of Education, Culture, Sports, Science, and Technology of Japan Grant-in-Aid for Scientific Research 20380188 (to N.K.).

## Author contributions

Y.N. performed most of wet experiments. K.M. performed nucleotide sequence analyses including RNA secondary structure prediction and prepared all figures. E.S. isolated *ire1a/ire1b* and performed phenotypic analysis of *ire1* mutants in Fig. 1. Y.S. performed microarray hybridisation, data collection and statistical analysis. Y.I. performed the



hierarchical cluster analysis of microarray data and wrote the manuscript. N.K. designed experiments, interpreted results and wrote the manuscript. All authors reviewed the manuscript.

### **Additional information**

Supplementary Information accompanies this paper at <http://www.nature.com/scientificreports>

**Competing financial interests:** The authors declare no competing financial interests.

**License:** This work is licensed under a Creative Commons Attribution-NonCommercial-ShareAlike 3.0 Unported License. To view a copy of this license, visit <http://creativecommons.org/licenses/by-nc-sa/3.0/>

**How to cite this article:** Nagashima, Y. *et al.* Arabidopsis IRE1 catalyses unconventional splicing of *bZIP60* mRNA to produce the active transcription factor. *Sci. Rep.* 1, 29; DOI:10.1038/srep00029 (2011).